We are IntechOpen,
the world's leading publisher of
Open Access books
Built by scientists, for scientists

4,800
Open access books available

122,000
International authors and editors

135M
Downloads

Our authors are among the

154
Countries delivered to

TOP 1%
most cited scientists

12.2%
Contributors from top 500 universities

CLARIVATE ANALYTICS
BOOK CITATION INDEX
INDEXED

WEB OF SCIENCE™

Selection of our books indexed in the Book Citation Index
in Web of Science™ Core Collection (BKCI)

Interested in publishing with us?
Contact book.department@intechopen.com

Development of a New 2 DOF Lightweight Wrist for the Humanoid Robot ARMAR

Albert Albers, Jens Ottnad and Christian Sander
IPEK - Institute of Product Development, University of Karlsruhe (TH)
Germany

1. Introduction

The mechatronic design of a humanoid robot is fundamentally different from that of industrial robots. Industrial robots generally have to meet requirements such as mechanical stiffness, accuracy and high velocities. The key goal for this humanoid robot is not accuracy, but the ability to cooperate with humans. In order to enable a robot to interact with humans, high standards are set for sensors and control of its movements. The robot's kinematic properties and range of movements must be adjusted to humans and their environment (Schäfer, 2000).

1.1 The Humanoid Robot ARMAR

The collaborative research centre 588 "Humanoid Robots – learning and cooperating multi-modal robots" was established by the "Deutsche Forschungsgemeinschaft" (DFG) in Karlsruhe in May 2001. In this project, scientists from different academic fields develop concepts, methods, and concrete mechatronic components for a humanoid robot called ARMAR (see figure 1) that can share its working space with humans.

Fig. 1. Upper body of the humanoid robot ARMAR III.

The long-term target is the interactive work of robots and humans to jointly accomplish specified tasks. For instance, a simple task like putting dishes into a dishwasher requires sophisticated skills in cognition and the manipulation of objects. Communication between robots and humans should be possible in different ways, including speech, touch, and gestures, thus allowing humans to interact with the robots easily and intuitively. As this is the main focus of the collaborative research centre, a humanoid upper body on a holonomic platform for locomotion has been developed. It is planned to increase the mobility of ARMAR by replacing the platform with legs within the next years, which will lead to modifications of the upper body.

1.2 State of the Art and Motivation

The focus of this paper is the design and the development process of a new wrist for the humanoid robot ARMAR. The wrist serves as the connection between forearm and hand. An implementation of the new modules is planned for the next generations of the humanoid robot, ARMAR IV and V. The wrist of the current version, ARMAR III, has two degrees of freedom (Albers et al., 2006) and its rotational axes intersect in one point. ARMAR III has the ability to move the wrist to the side (± 60°, adduction/abduction) as well as up and down (± 30°, flexion/extension). This is realized by a universal joint in a compact construction. At the support structure of the forearm all motors for both degrees of freedom are fixed. The gear ratio is obtained by a ball screw in conjunction with either a timing belt or a cable. The load transmission is almost free from backlash. The velocity control and the angular measurement in the wrist are realized by encoders at the motors and by quasi-absolute angular sensors directly at the joint. To measure the load on the hand, a 6-axis force and torque sensor is fitted between the wrist and the hand.

One of the main points of criticism on the current version of the wrist is the offset between the rotational axes and the flange, as shown in figure 2 (left). Due to the joint design, this offset distance is necessary in order to provide the desired range of motion. Also other wrists of humanoid robots show a similar design, see (Shadow), (Kaneko et al., 2004), (Park et al., 2005), (Kaneko et al., 2008). That offset is even greater due to the placement of the 6-axis force and torque sensor. The resulting movement, a circular path performed by the carpus, does not appear as a humanlike motion, as illustrated in figure 2 (right).
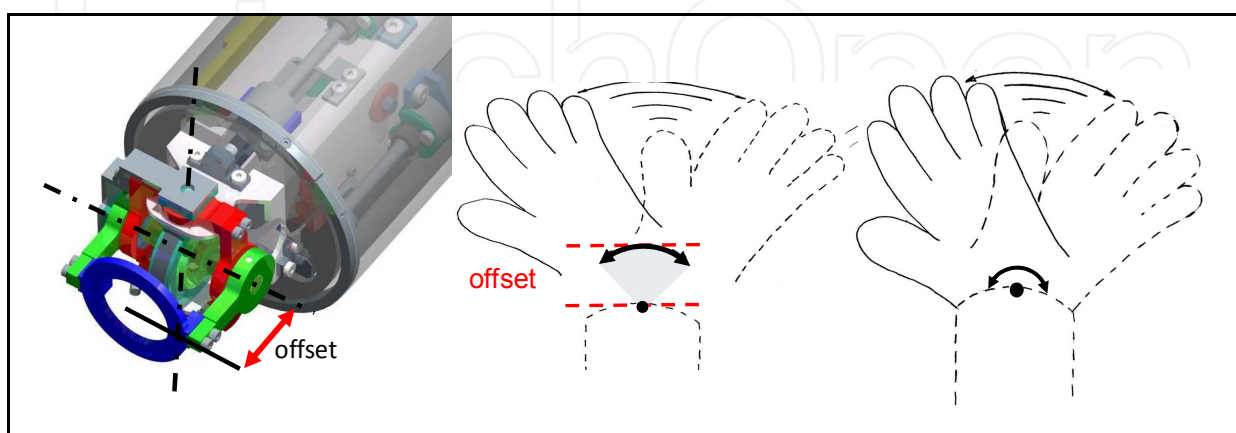

Fig. 2. Offset between the rotational axis and the hand flange at the wrist of the humanoid robot ARMAR III (left) and the resulting movement (right)

The German Aerospace Centre DLR (Deutsches Zentrum für Luft- und Raumfahrt) has been working on seven degree of freedom robot arms for several years. The result of this project is shown in figure 3 (left). Although their work is inspired by a human arm, their goal is not to design humanoid robots. The wrists of the lightweight arms of the third generation imitate human wrist movements by a pitch-pitch combination with intersecting axes (kardanic). An alternative pitch-roll configuration is also utilized, mainly for applications using tools (Albu-Schäffer et al., 2007). Both versions have an offset comparable to the current wrist of ARMAR III.

Henry J. Taylor and Philip N.P. Ibbotson designed a so called "Powered Wrist Joint" (Rosheim, 1989) in order to load and unload space shuttles. The concept of this wrist is illustrated in figure 3 (right). In a smaller version, the basic idea could be reused in humanoid robot's wrist. The second degree of freedom (pitch) of the wrist is guided by a spherical joint. Such an assembly provides a slim design and relatively wide range of motion. The actuators for the second degree of freedom (yaw) are located directly at the joint; therefore, the drive units are quite simple. On the other hand, miniaturization seems to be very difficult due to the dimensions of common gears and motors.
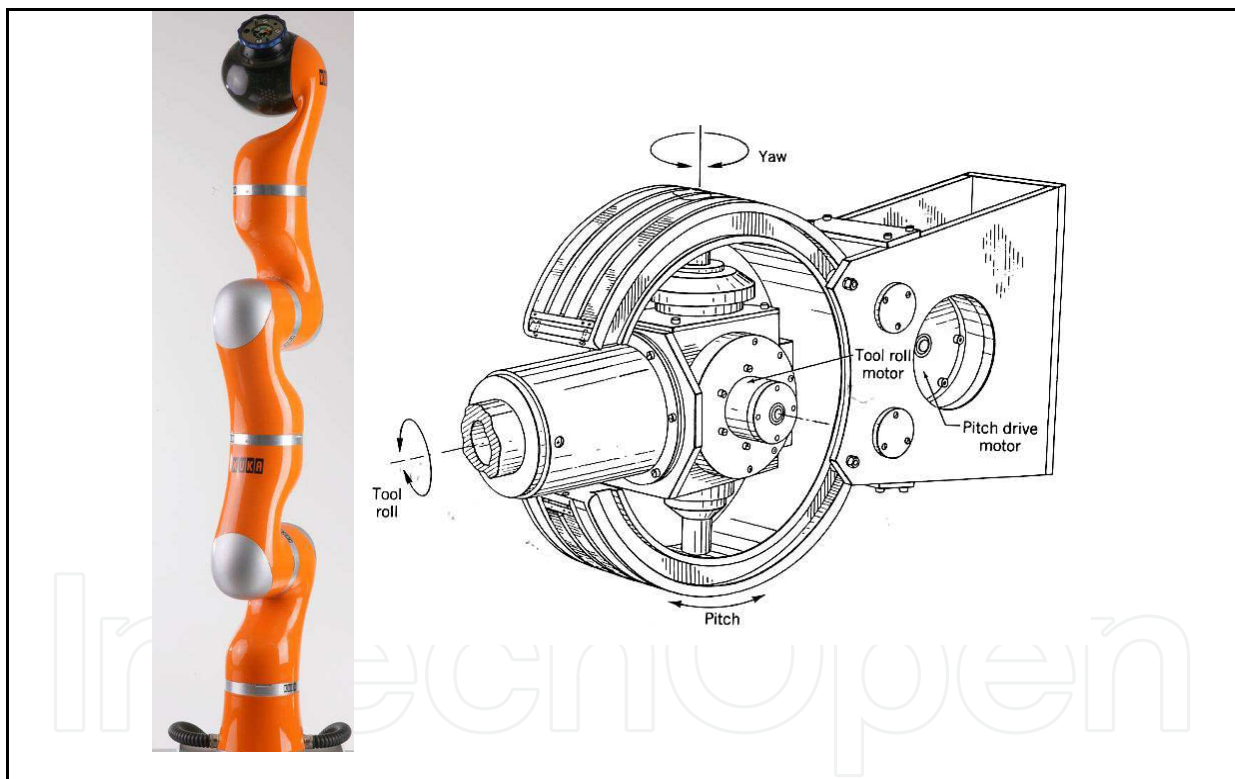

Fig. 3. The DLR/Kuka lightweight robot arm (Abu-Schäfer et al. 2007) (left) and concept for a wrist actuator (Rosheim, 1989) (right).

2. New Concept

2.1 Requirements and Design Goals
In this section the system of objectives is defined. It describes all relevant objectives, their dependence and boundary conditions, which are necessary for the development of the correct object system, outgoing from the current condition to the future condition. But the

solution itself is no part of the system of objectives. It is permanently extended and concretized over the complete product lifecycle. The correct, consistently and complete definition of this system is the basis of the successful product development and a core component of the development activity (Albers et al., 2008a). Since the robot is intended to get in contact with humans in order to achieve various functions, it is inevitable that the robot is accepted by the human. The ability to move like a human is as important as a human-like appearance; therefore, specific demands (Asfour, 2003) on kinematics, dynamics and the design space must to be considered. A human wrist consists of many different elements and has a relatively wide range of motions. Figure 4 illustrates the different possible movements of the human wrist along with the corresponding reachable angular position of the joints (Whired, 2001).
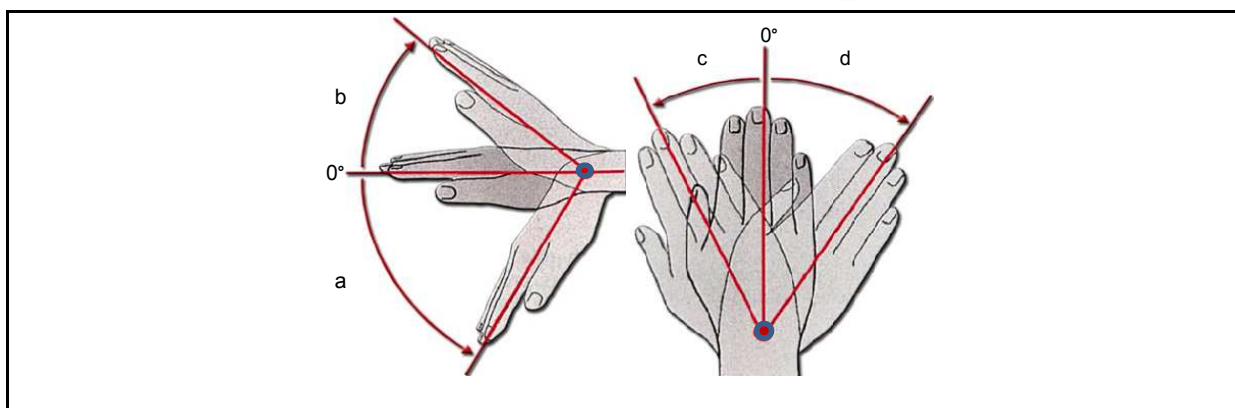

Fig. 4. Human wrist and range of motion: a = palmar flexion 70°, b = dorsal flexion 90°, c = radial abduction 20°, d = ulnar abduction 40° (Whired, 2001).

In order to implement a human-like wrist movement, two orthogonally arranged rotational degrees of freedom are necessary. Both axes are orthogonal to the forearm's axis and intersect in one point. The two degrees of freedom need to be put in a kinematical series.

The requirements and design goals for a humanoid robot's wrist can be deduced based on the range of motion of the human wrist. The first degree of freedom should have a ±30° range of motion and the second about ±90°. The wrist will be attached to the forearm's structure on one side and provides the connection to the hand. It should be possible to disconnect the mechanical joint between the hand and wrist in a simple way in order to enable a modular design. To measure the load on the hand, a 6-axis force and torque sensor must be fitted between the wrist and the hand. The electronic cables and pneumatic tubes supplying power to the hand actuators are the similar to those used in the previous models of ARMAR (Schulz, 2003; Beck et al., 2003). The design space for the robot's wrist is based on human dimensions as far as possible; therefore, one aim is to keep a sphere of approximately 100 mm in diameter as a boundary. At the same time, the control strategy aims to operate all degrees of freedom as individually as possible.

In keeping with the standardized drive concept of most modules of the robot, electronic motors are used as the source for actuation. The drive units need to be dimensioned for a load of 3 kg. All gears are designed to be free from backlash and not self-locking. But friction, e.g. in case of a loss of power, leads to a slow and damped sinking of the arm instead of abrupt movement. That is of great importance for an interactive application of the

robot in a human environment. On the other hand, stick-slip effects in the gears have been avoided, which is a clear benefit for the control system.

Finally, the mechanical structures should be as light as possible in order to save energy during dynamic movements. A lower mass of the wrist can contribute significantly to a reduced energy consumption of the whole arm and has a strong influence on the gears and motors used for the drive units for the elbow and shoulder degrees of freedom.

2.2 Concepts

A simple reduction of the wrist's length by only minor modifications is not possible. This is mainly because the current joint design in combination with the drive unit for the second degree of freedom does not allow a mounting of the hand in the rotational axis. Formulated in an abstract way, the development goal is to shift material from the intersection point to a different location in order to gain free space in the centre position.

Bodies in general have six degrees of freedom in a three dimensional space: three rotational, and three translational. Due to design complexity, the degrees of freedom must be reduced for the development of a technical joint. As technical solutions in robotics usually have only one degree of freedom, it is necessary to combine two basic joints to implement a two degree of freedom joint (Brudniok 2007). An alternative solution is a spherical joint where one rotation is blocked, but actuators for such a design have not yet been sufficiently developed. As result of these basic considerations, two principle solutions were found: a universal joint and a kind of curved track as depicted in figure 5.
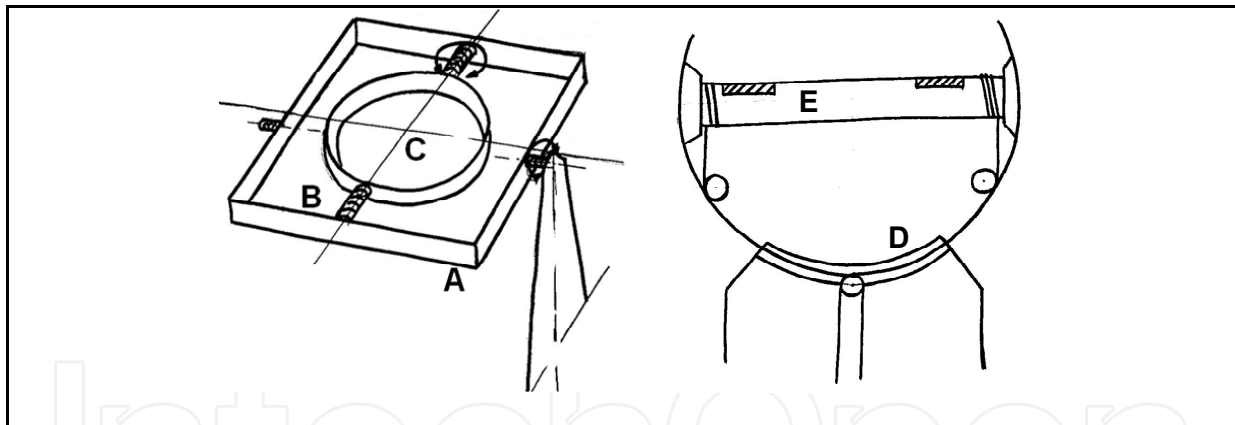

Fig. 5. Universal joint (left) and the principle curved track solution (right).

To illustrate the decision process within the development both concepts are discussed shortly. The universal joint concept (figure 5 left) is very similar to the current solution running on ARMAR III. The first degree of freedom is provided by a rectangular frame (A). On that frame there is enough space for the bearings (B) of the second degree of freedom. Finally, the hand can be mounted on the plate (C). In contrast to the current version, the reduced length was achieved by taking all elements in one plane. The disadvantage is that the outer diameter has to be enlarged in order to provide the wide range of motion described in the previous section. One possible implementation of the drive units could be a direct connection by bowden cables providing a slim and light design of the joint itself. By applying this idea to the universal joint, the total length (TL) of each cable changes. Figure 6 illustrates the parameters which are of importance for a two dimensional consideration.
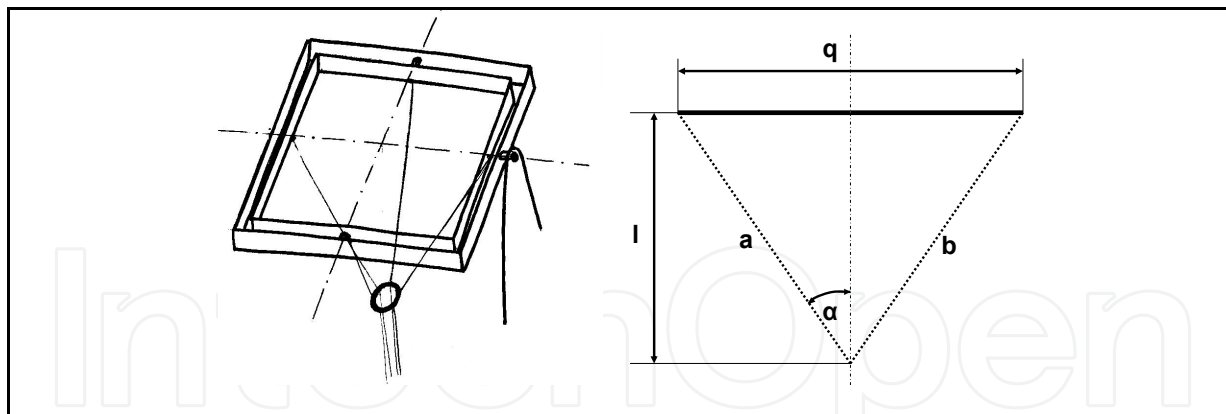
Fig. 6. "Changing" length of the cables in different angular positions of the wrist.

The total lenght can easily be calculated by the following formula, where α denotes the angle between the cables and the middle axis of the forearm:

$$TL = a + b = 2 \cdot \frac{l}{\cos(\alpha)} \tag{1}$$

As α depends on the angular position of the wrist, TL changes during each movement. That means that the different degrees of freedom can not be run independently as long as electronic motors are used as actuators. The Shadow Hand, for example, uses a different concept concerning the cables and their changing lengths (Shadow).

The second basic concept depicted in figure 5 on the right side consists of a curved track solution for the first degree of freedom (D). As this first rotation is limited to ±30°, there is enough space left for the bearings of the second degree of freedom, which may be realized, e.g., by a simple shaft (E). This configuration allows a relatively wide range of motion and a high capability for a reduction of the wrist's length. The challenges for this concept include finding a technical solution for the curved track, a suitable actuation and a design with a proper stiffness in the structures.

Overall, both basic concepts fulfill the principle requirement of length reduction. The curved track method, however, has a clear advantage in terms of size in the radial direction. The oval outer contour also shows a better similarity to a human wrist; therefore, the curved track concept was selected for further development.

2.3 Embodiment Design

By an appropriate design of the shaft (see figure 5 right, named E) it is possible to gain still more space for the 6-axis force and torque sensor. Figure 7 illustrates a cross-section view of the modified shaft. The depth of the shell corresponds with the radius of the curved track and enables a mounting of the hand exactly in the point where the rotational axes intersect. This is achieved by shifting the mechanical connection in the negative direction along the center axis of the forearm.
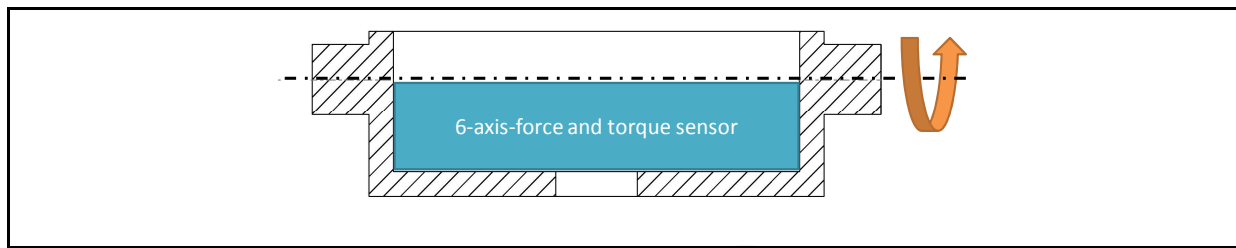
Fig. 7. Basic idea for the shaft of the second DOF of the wrist integrating the force sensor.

For the technical implementation of the curved track, a curved guide named HCR manufactured by THK was selected. Used for medical applications, THK produces ceramic curved guides with a radius of approximately 100 mm. From a technical standpoint it would have been possible to reduce the radius to meet the requirements for a humanoid robot's wrist. For economic reasons, however, this was not a feasible option for the collaborative research centre. Therefore, a different solution was necessary.

The curved guide was replaced by rollers in combination with a timing belt. This allowed the integration of two different functions in one element: the timing belt functions as part of the drive unit while also providing sufficient pre-load to avoid a gap between the rollers and the track. Figure 8 shows the basic CAD model of each design.
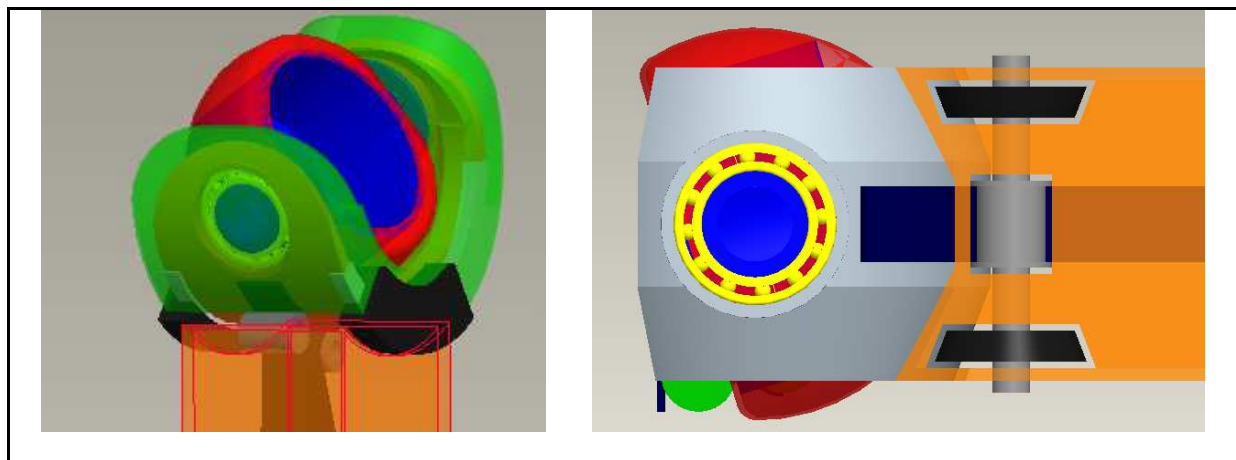

Fig. 8. First technical solution by using a curved guide (left) and the alternative using a roll timing belt combination (right).

3. Simulation

3.1 Basic Geometric Considerations

Based on the new concept an analytic model can be set up. Therefore all geometrical parameters based on the nature of the human body have to be adapted to the model. The undefined variables have to be calculated and estimated using the analytical model to get a reasonable set of values for the design. Using parameter optimization the best combination of values for a design proposal can be found in order to achieve reasonable preloads for the belt.

Two main load cases were used whereas the angle of the initiated force φ can vary. Figure 9 illustrates these two load cases. Here the calculated force F (36 N) is the substitute for all external loads and self-weight (Albers et al., 2006). M is the appropriate torque resulting

from the arm of lever and is about 3.14 Nm. To avoid a displacement of the cap the preload F_V has to be chosen great enough
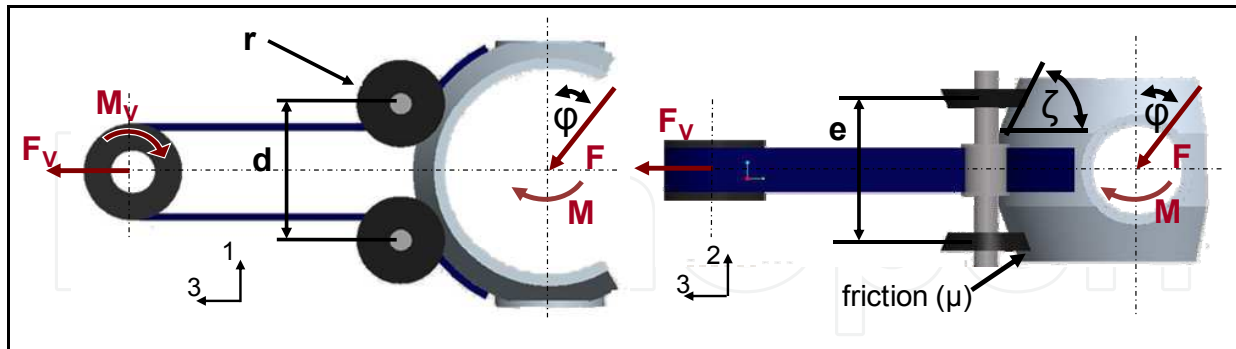

Fig. 9. Load case I (left) and load case II (right) in two different directions.

Load case I:
The external load F is applied in a variable angle φ towards the vertical line. The maximum required preload for an offset of the beveled wheels (d) of 37.5 mm is about 1 kN. When d is increased to 42.5 mm, the required force is less than 0.63 kN. Thus, the required force decreases by about 37 % when the off-set of the beveled wheels is increased by about 21 %. By doubling the distance from 35 mm to 70 mm, the required preload force is reduced by 90 %. The calculated critical angle of the load φ is 36°.

Load case II:
Calculations have shown that the influence of the substituted shear force F is negligible for this load case. Therefore only the over-all torque M is used for the analysis. F_V is dependent upon the angle ς and the wheel distance e. The calculated maximum force for the timing belt is 0.28 kN. The calculated forces are all in a reasonable range compared to the technical elements that can be used for the construction. Consequently the concept can be realized in a physical system with standard bearings and materials.

3.2 First Design and Finite Element Analysis
On the basis of the analytic results described in section 3.1, the optimal solution for the free geometrical parameters can be defined and in a further step be designed in a CAD system. An impression of the parameter optimized wrist is given in figure 10:
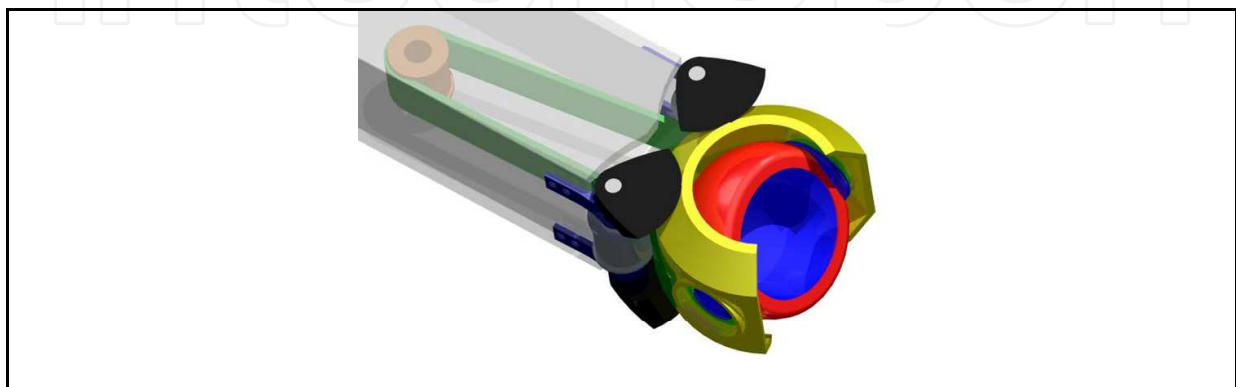

Fig. 10. CAD model based on the results of the analytical considerations.

In a next step the CAD model is simulated numerically using Finite Element Method (FEM) in order to gain further information of the system's behavior. Especially the elasticity of the different structures and the resulting interaction effects are of interest. The preload force and the orientation of the external force were varied systematically. The primary object is to get values for the displacement of the cap towards the global coordinate system. ABAQUS (Dassault Systèmes) is the used solver for the FEM. In order to reduce the computing time, the CAD model must be simplified while the fundamental behavior of the system should be modeled as accurately as possible. The following parts are taken into account for the Finite Element Analysis (FEA): The cap, the beveled wheels, the idler and the timing belt are modeled as deformable with the ABAQUS- element type 'C3D8I' (except beveled wheels, C3D8R). Analytical rigid elements are used for the connecting wheels and the driving shaft. All deformable parts are simulated with isotropic material except the timing belt. Due to the fact that the timing belt is composed of a steel cord with polyurethane backing and teethes, an anisotropic material parameter is used in the model. The angle φ of the external load takes the value of 0° and 36° which is identified in the analytic calculation as the most critical. Figure 11 illustrates the result of the FEA.
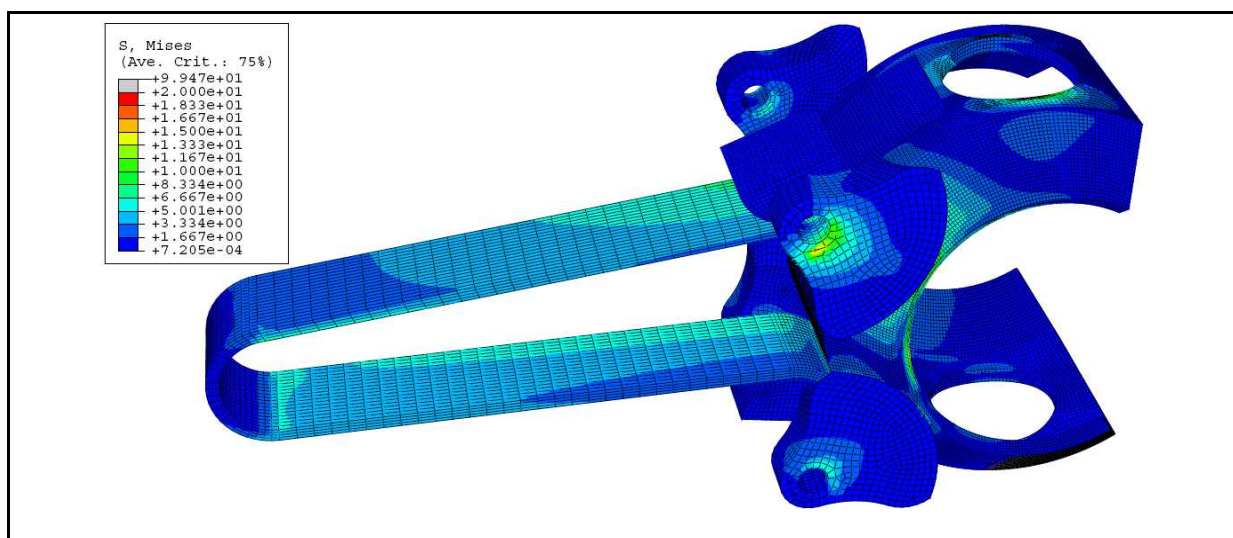

Fig. 11. Stress distribution (von-Mises criterion) for load case II.

The stresses, obtained by the FEA show a reasonable distribution. The displacement of the cap tested with high preload forces is minimal due to the FEA. For a preload of 0.6 kN the displacement for load case II is about $4.4 \cdot 10^{-3}$ mm and for load case I $1.39 \cdot 10^{-2}$ mm. Compared with a preload of 1 kN the displacement doesn't highly decrease. For load case II the displacement takes the value of about $4.07 \cdot 10^{-3}$ mm and for load case II $1.29 \cdot 10^{-2}$ mm. These values for the different preloads show that in the range between F_V=0.6 and 1.0 kN only a small increase of positioning accuracy due to less displacement can be reached. But the high additional costs in the construction of the wrist for preloads higher than 0.6 kN can't be justified. For this reason, and for practical implementation, it is not meaningful to use forces greater than 0.6 kN. For preloads lower than 0.25 kN the position deviation increases dramatically and the system becomes statically indeterminate. The displacement of load case I with φ=36° is for every point smallest compared with load case I (φ=0°) and

load case II. Therefore, it appears that a preload between 0.25 kN and 0.6 kN would be most suitable.

4. Functional Prototype

Based on the positive results obtained by the different simulations, a functional prototype was developed. That was necessary mainly because different functions were integrated in the toothed belt, which is usually used in a different manner and not all material parameters were available so that estimated values were used.

As the purpose of the prototype is to prove basic functionality of the design, a few simplifications are made. For the beveled wheels complete rolls are used and the cap is designed in a simple way for instance. Further-more, the construction allows the possibility to implement an s-beam force sensor (Lorenz K-25). Figure 12 shows two pictures of the assembled functional prototype with a one kilogram weight attached at the hand's position.
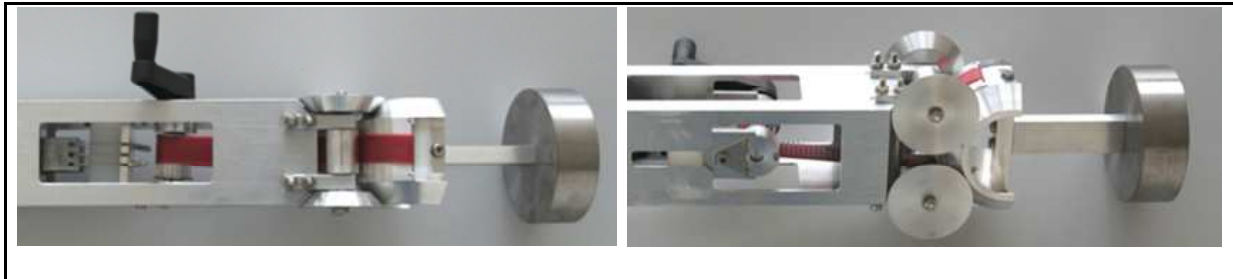
Fig. 12. Functional prototype.

Multiple static and dynamic tests show that this configuration is very accurate and has a high stiffness for small preloads of about 300 N. Hereby the wrist is hand-held at the forearm tube and statically loaded by huge forces between 20-80 N or moved dynamically in all different directions. Even for very fast "hand actuated" motions, which were approximately five times of the maximum velocity of the robot's arm, the assembly remained free from backlash.

5. Optimization and Lightweight Design

As a lightweight design is one of the main goals for the development of the new wrist, different numerical optimization methods were used.

5.1 Topology Optimization

Topology optimization is used for the determination of the basic layout of a new design. It involves the determination of features such as the number, location and shape of holes, and the connectivity of the domain. A new design is determined based upon the design space available, the loads, possible bearings, and materials of which the component is to be composed. Today topology optimization is very well theoretically studied (Bendsoe & Sigmund, 2003) and also a common tool in the industrial design process (Pedersen & Allinger, 2005). The designs, obtained using topology optimization are considered as design proposals. These topology optimized designs can often be rather different compared to

designs obtained with a trial and error design process or designs obtained from improvements of existing layouts. The standard formulation in topology optimization is often to minimize the compliance corresponding to maximize the stiffness using a mass constraint for a given amount of material. That means that for a predefined amount of mass the structure with the highest stiffness is determined. Compliance optimization is based upon static structural analyses, modal analyses or even non-linear problems, such as models including contacts. A topology optimization scheme is basically an iterative process that integrates a finite element solver and an optimization module. Based on a design response supplied by the FE solver (e.g. strain energy), the topology optimization module modifies the FE model.

5.2 Material Optimization

Besides the topology optimization, it is necessary in addition to consider optimization strategies such as material optimization. Extreme lightweight design is possible only by combining both optimization strategies such as the topology optimization in combination with an optimal fiber layout. For calculation of laminates by use of the Finite Element Method (FEM), approaches are used that combine the properties of single plies to one virtual material by use of the 'Classical Lamination Theory' (CLT) (Johns, 1999). These established theories are valid for the elastic range.

Several approaches for the determination of optimal fiber orientation have been presented in the past. (Luo & Gea, 1998) use an energy based method. (Setoodeh, 2005) describes an optimality criteria approach, while (Jansson, 2007) works with a generic algorithm. Inspired by nature (Kriechbaum 1994), (Hyer & Charette, 1987) place fibres in direction of first principal stress. In that context (Lederman, 2003) presents a method placing the fibers in the direction of the first main stress in the finite element. (Pedersen, 1991) showed, that a fiber orientation according to the first main strains leads to maximization of stiffness. Most of those approaches only work for one layer, and are reduced on two dimensional problems.

The method used in that work was developed by (Albers et al., 2008b), focusing two main goals: Fast convergence, because the approach is intended to be used together with FEM, and, in a second step, combination with topology optimization. Application should be possible for 3D-geometries, and determination of a two layered laminate structure (orientation and thicknesses) had to be possible to take multi-axial load cases into account. The approach is based on a theory described by (Ledermann, 2003). Optimal fiber orientation is found, if it is equal to the orientation of the first main stress. To be able to take multi-axial load cases into account, the method creates two plies per finite element, with the second ply oriented in the direction of the second main stress. The relation of thickness of the two plies is proportional to the relation of the two main stresses. The orientation of the composite in space is defined by the surface created by the two directions of the main stresses. The third main stress is not taken into account, because 3-dimensional canvases are normally not used in real world applications.

The method is implemented in an iterative procedure, starting with a finite element model with isotropic material. Thenceforward, the isotropic material model is replaced by an anisotropic one with the parameters of a combined two-layer composite. Stress and ply directions are updated in every iteration. In detail, the following steps are undertaken in each iteration: From the preceding finite element analysis, main stress directions and -amounts are determined for each finite element. The procedure starts with the

transformation of the direction vectors of main stresses from the element coordinate systems to the vector of the global system by use of the direction cosines. The cross product of the direction vectors of the two first main stresses is used to define the perpendicular to the later surface of lamina of the element. In the special case of the cross product being the zero-vector, e.g. the uniaxial stress condition, a filter is used to determine the perpendicular out of the neighboring elements. By use of the given engineering constants $E_\parallel$, $E_\perp$, $\upsilon_{\perp\parallel}$, $\upsilon_{\perp\perp}$ and $G_{\perp\parallel}$ of the chosen fiber-matrix-combination, the orthotropic stiffness matrix $[C]$ of the UD-layers can be reduced to a transversal isotropic one as follows:

$$[C] = \begin{bmatrix} C_{11} & C_{12} & C_{13} & 0 & 0 & 0 \\ C_{21} & C_{22} & C_{33} & 0 & 0 & 0 \\ C_{31} & C_{32} & C_{33} & 0 & 0 & 0 \\ 0 & 0 & 0 & C_{44} & 0 & 0 \\ 0 & 0 & 0 & 0 & C_{55} & 0 \\ 0 & 0 & 0 & 0 & 0 & C_{66} \end{bmatrix} \tag{2}$$

with

$$C_{11} = \frac{1-\upsilon_{23}\upsilon_{32}}{E_2 E_3 \nabla}, \; C_{22} = \frac{1-\upsilon_{13}\upsilon_{31}}{E_1 E_3 \nabla}, \; C_{33} = \frac{1-\upsilon_{12}\upsilon_{21}}{E_{21} E_1 \nabla}$$

$$C_{12} = \frac{\upsilon_{12}+\upsilon_{32}\upsilon_{13}}{E_1 E_3 \nabla}, \; C_{13} = \frac{\upsilon_{13}+\upsilon_{12}\upsilon_{23}}{E_1 E_2 \nabla}, \; C_{23} = \frac{\upsilon_{23}+\upsilon_{21}\upsilon_{13}}{E_1 E_2 \nabla} \tag{3}$$

$$C_{44} = C_{23}, \; C_{55} = C_{13}, \; C_{66} = C_{12}$$

and

$$\nabla = \frac{1-\upsilon_{12}\upsilon_{21}-\upsilon_{23}\upsilon_{32}-\upsilon_{31}\upsilon_{13}-2\upsilon_{21}\upsilon_{32}\upsilon_{13}}{E_1 E_2 E_3} \tag{4}$$

Now, the engineering constants mentioned above are introduced:

$$E_2 = E_3 = E_\perp$$

$$G_{31} = G_{21} = G_{\perp\parallel}$$

$$\upsilon_{31} = \upsilon_{21} = \upsilon_{\perp\parallel} \tag{5}$$

$$G_{\perp\perp} = \frac{G_{\perp\parallel}}{2(1+\upsilon_{\perp\perp})}$$

The angle α between the two layers is the angle between the two first main stresses. It can be obtained by use of the direction cosines. The volume share of the two layers is calculated as:

$$\upsilon_1 = \frac{|\sigma_1|}{|\sigma_1| + |\sigma_2|} \, , \; \upsilon_2 = 1 - \upsilon_1 \tag{6}$$

By use of the 'Classical Lamination Theory' (CLT), the combined stiffness matrix [C_{com}] of the two-layer-lamina can now be calculated. First, the stiffness matrix of the smaller layer is transformed into the lamina coordinate system, defined by the direction of the first main stress. This is done by rotating the stiffness matrix of the layer [C]' about α:

$$[C] = [T]^{-1} [C][T]^{-T} \tag{7}$$

With [T] the following transformation matrix:

$$[T] = \begin{bmatrix} \cos^2 \alpha & \sin^2 \alpha & 2\sin\alpha\cos\alpha \\ \sin^2 \alpha & \cos^2 \alpha & 2\sin\alpha\cos\alpha \\ -\sin\alpha\cos\alpha & \sin\alpha\cos\alpha & \cos^2 \alpha - \sin^2 \alpha \end{bmatrix} \tag{8}$$

The combination of the two layers is done by use of the rules defined by the CLT. The iteration is finished by formatting and writing the new anisotropic stiffness matrices in the input deck for the FEA. Depending on the FE code used, the materials has to be filtered and clustered before a FEA can be performed, as some FE algorithms are limited in the number of materials allowed. Reduced convergence speed and accuracy of the approach may result.

5.3 Model Setup

For the topology and material optimization the complete system is disassembled and only the cap is used for the optimization. This simplification is necessary to avoid enormous computing time caused by a very fine mesh for the cap and a huge number of load cases. Cutting these parts free from the total system, calls for a realistic replacement of the interaction between the components. Hereby the interaction between the beveled wheels and cap is replaced by a connection at the corresponding nodes which allows a degree of freedom in the 3-axis direction. This simplification is possible because the appearing forces can only be compressive force or the cap lifts off the wheel surface. The timing belt is replaced by a load which is tangential to the cap and transferred to the structure by 5 points on each side of the cap. The preload used in place of the timing belt is 450 N. On one side of the cap an additional force is applied to the timing belt which is the result of an inertial relief and named $F_{inertrel}$. The external load (F) is defined to 30 N and applied to the cap by a torsion arm, which is modeled as rigid element (RBE in MSC.Nastran), in a distance of 100 mm in negative 3-coordinate-axis. The force vector can be reduced to three different directions because of the symmetry conditions can be defined for the optimization process.

The additional torque (M) represents 5 Nm and rotates about the global 3-coodrinate-axis. In figure 13 eight different load cases are illustrated.
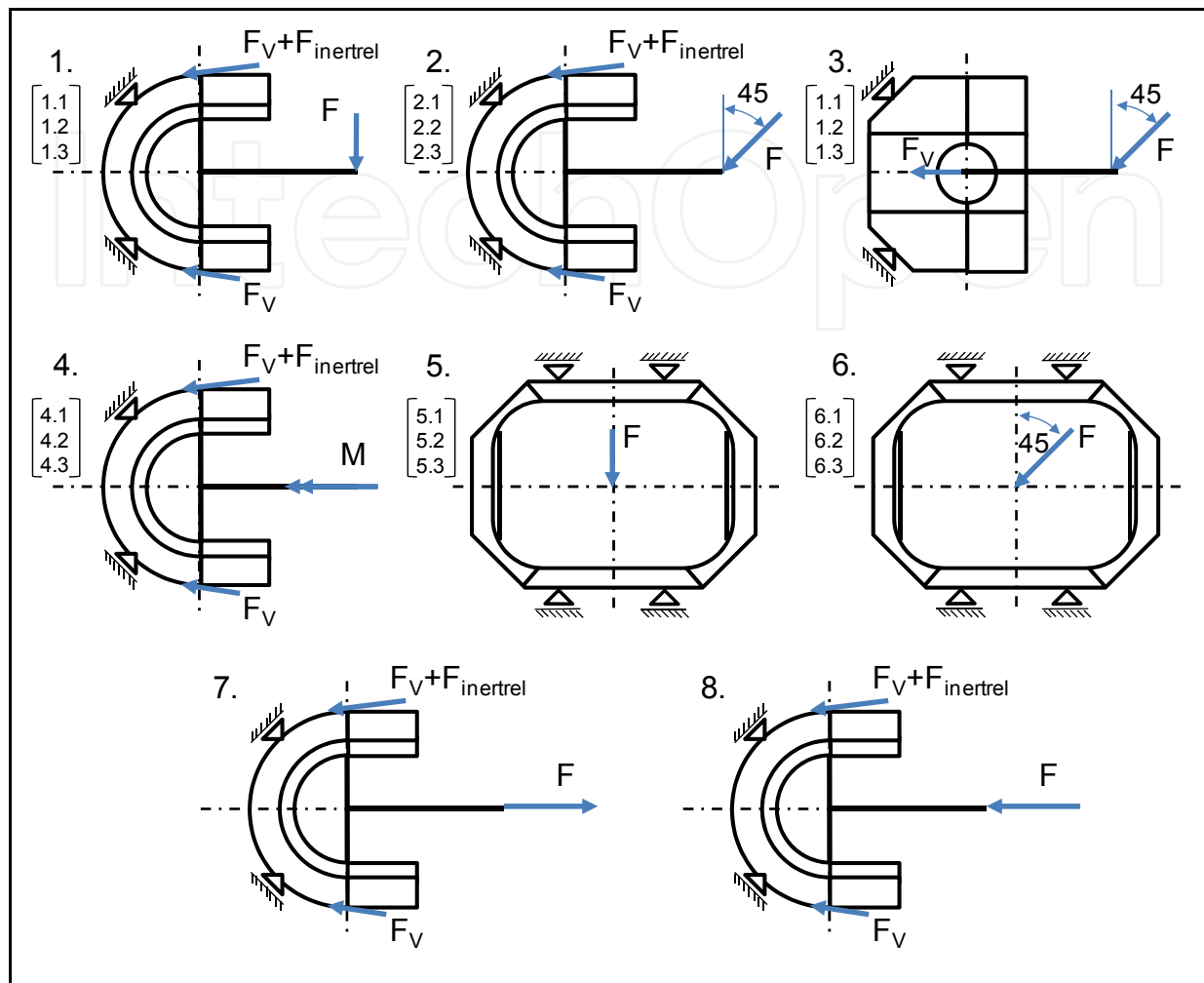

Fig. 13. Load cases for the topology optimization.

The first six load case combinations are set for three different rotational positions of the second DOF. The initial state is the neutral position and two other positions are realized by changing the direction and position of all forces on the cap as they would appear at a ±30° rotation. From this it follows that 18+2=20 different configurations of the cap are set for the topology optimization.

5.4 Results

The result of the topology optimization as a basic design proposal is shown in figure 14. The complex topography in the center is a result of the stress caused by the torsional moment applied to the structure mainly by load case 4 (4.1, 4.2, 4.3). The direct connection to the bearing by the beveled wheels is visible clearly. The function of the center link is mainly to absorb the reaction forces applied to the cap by the high preload and the beveled wheels. The side links are important to reinforce the cap structure between the two points of force

transmission of the timing belt. The shape of an arrowhead as a result of the two side links is highlighted on the right side in figure 14.
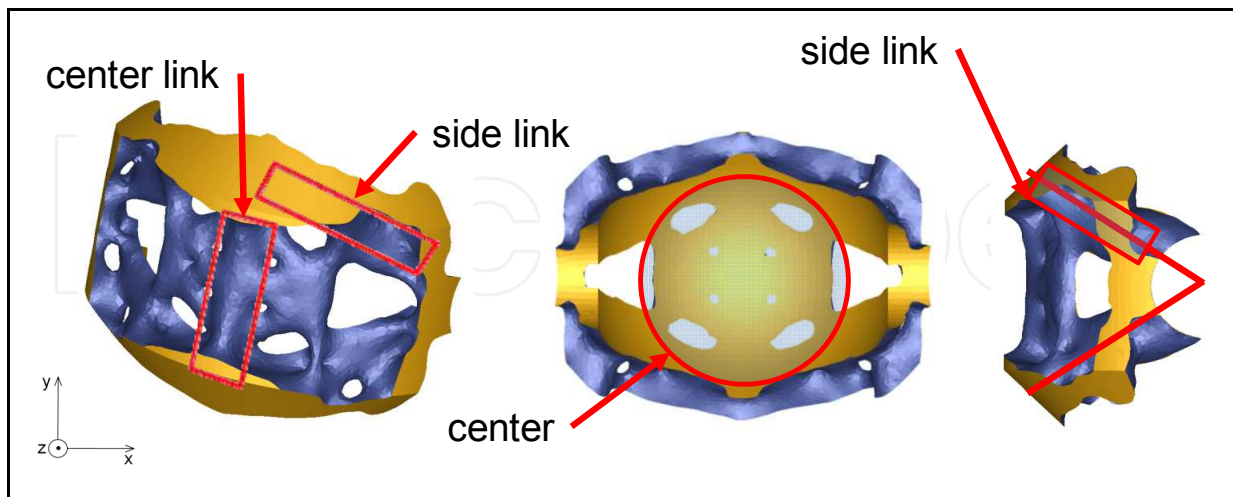

Fig. 14. Smoothed design proposal as a results by the optimization for a lightweight laminate.

In figure 15 the principle stress for an anisotropic topology optimization is illustrated. The highlighted regions are areas with preferred orientated principle stress, which is important while using fiber reinforced materials. Furthermore the stress is uniaxial in these regions. A zoomed view (round clippings) clarifies the stress orientation. In these regions the fibers in the laminate can be orientated in the direction of the principle stress which on the one hand reduces the amount of used material and by that the weight of the cap and on the other hand it improves the stiffness and accuracy. Regions which are not highlighted have changing stress orientations and different stress states. In these areas laminates have to be stacked with different orientations to absorb the multiaxial stress.
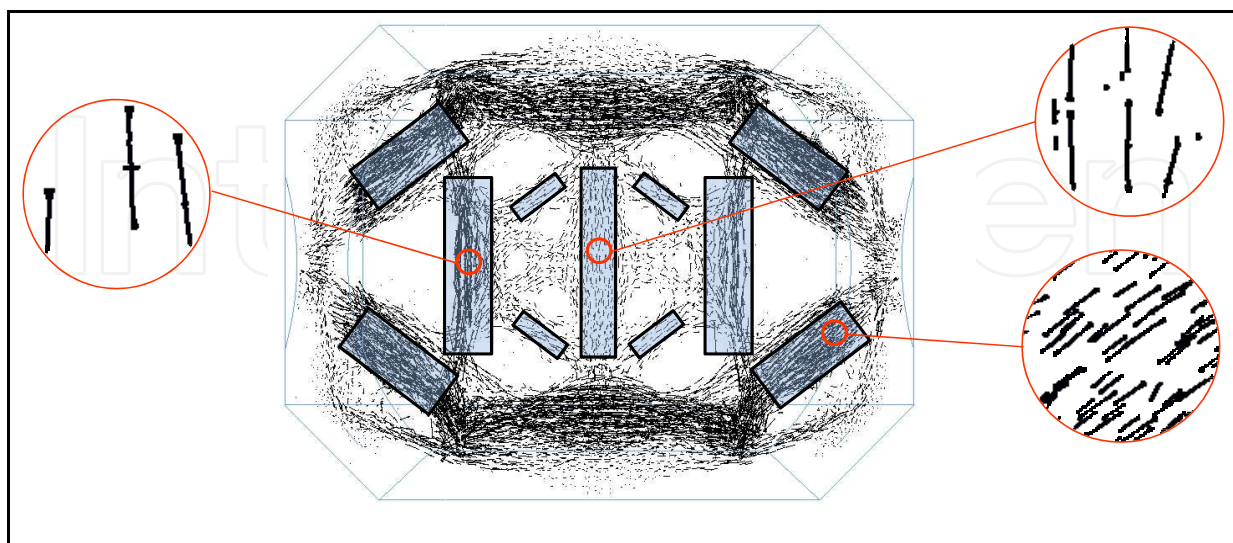

Fig. 15. Principle stress highlighted for a laminate.

Based on the optimization results a 3D-CAD model can be implemented as a first design proposal (see figure 16). In order to realize a lightweight design, the part is built up as an hollow shell. The advantage is that the material is located at the outer area which increases the bending stiffness. To reduce the comprehensive stress at the friction contact zone where the beveled wheels are crawling, a metal band is laminated into the fiber composite. This metal band also increases the stiffness. Furthermore compression proof foam can be integrated into the shell in areas with high pressure mainly introduced to the structure by high preloads. The complex suggestion for the center by the topology optimization is reduced to a thickened center link. To big holes in the structure reduce the weight. In figure 16 on the right side the arrowhead shape, which was suggested by the optimization, is visible. This shape allows a good distribution of forces within the structure.
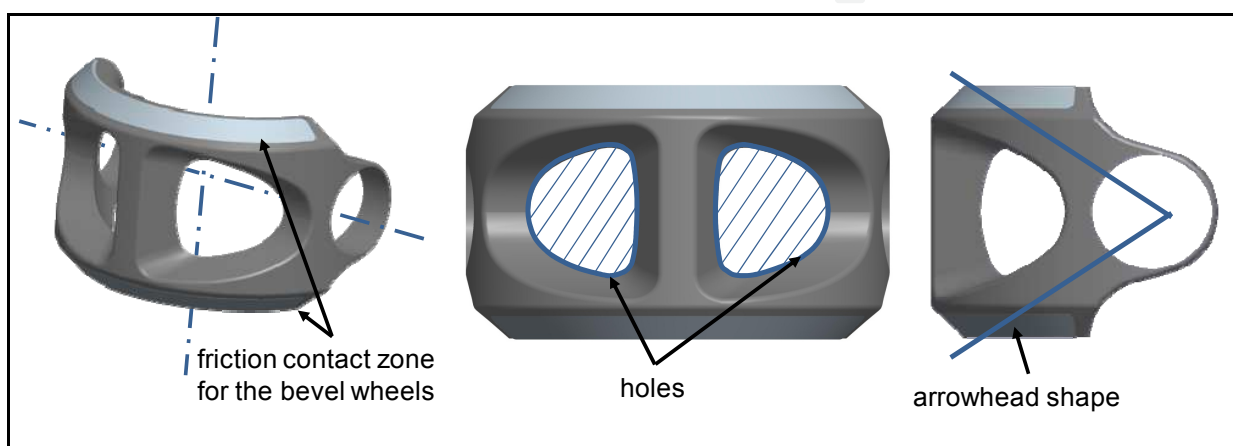

Fig. 16. 3D-CAD model of a design proposal.

Due to the two holes in the structure a new concept for the timing belt is required. Therefore two narrow belts instead of one are used to apply the preload to the cap. In figure 17 a 3D-CAD model with a suggestion for the two timing belts is illustrated. This arrangement increases the support effect and results in a better positioning accuracy.
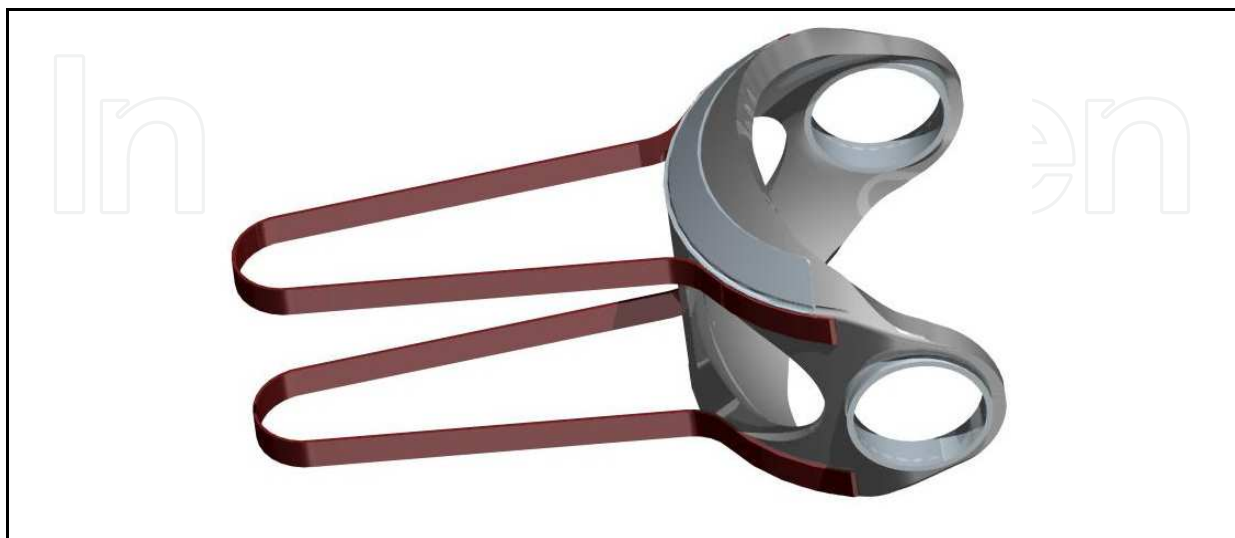

Fig. 17. 3D-CAD model of a design proposal for the timing belt.

6. Conclusion

In this paper the development of a new concept for humanoid robot's lightweight wrist is presented. Especially the different steps of the development process are described. Based on the basic ideas, different analyses and simulations are conducted. A functional prototype is presented which is a kind of proof of the concept. Due to the design proposal obtained by the topology optimization for a fiber composite, a lightweight design is implemented in the CAD model.

The next step will be the integration of the drive units for the second degree of freedom. Here different solutions are possible, e.g. like bowden cables or a direct actuation in combination with harmonic drive gears. In order to achieve a further reduction of mass, composite materials may be used for some further of the structural components. The new wrist will be developed in the next months and is to be manufactured and assembled during the next year.

7. References

Albers A.; Brudniok S.; Ottnad J.; Sauter Ch.; Sedchaicharn K. (2006) Upper Body of a new Humanoid Robot – the Design of Armar III, *Humanoids 06 - 2006 IEEE-RAS International Conference on Humanoid Robots*, December 4 to 6, 2006 in Genova, Italy.

Albers, A.; Deigendesch, T.; Meboldt, M. (2008a). Handling Complexity – A Methodological Approach Comprising Process and Knowledge Management, *Proceedings of the TMCE 2008, 2008 TMCE International Symposium on Tools and Methods of Competitive Engineering*, April 21-25, 2008, Izmir, Turkey.

Albers, A.; Ottnad, J.; Weiler, W. (2008b). Integrated Topology and Fibre Optimization for 3-Dimensional Composites, *Proceedings of IMECE 2008, 2008 ASME International Mechanical Engineering Congress and Exposition*, November 2-6, 2008, Boston, Massachusetts, USA.

Albu-Schäffer, A.; Haddadin, S.; Ott, Ch.; Stemmer, A.; Wimböck, T.; Hirzinger, G. (2007). The DLR lightweight robot: design and control concepts for robots in human environments, *Industrial Robot: An International Journal*, Vol. 34 No. 5, 2007.

Asfour, T. (2003). *Sensomotorische Bewegungskoordination zur Handlungsausführung eines humanoiden Roboters*, Dissertation Fakultät für Informatik, Universität Karlsruhe, 2003.

Beck, S.; Lehmann, A.; Lotz, Th.; Martin, J.; Keppler, R.; Mikut, R. (2003). Model-based adaptive control of a fluidic actuated robotic hand, Proc., *GMA-Congress 2003*, VDI-Berichte 1756, S. 65-72; 2003.

Bendsoe, M. & Sigmund, O. (2003). *Topology Optimization – Theory, Methods, Application*, Springer Verlag 2003.

Brudniok, S. (2007). Dissertation - Methodische Entwicklung hochintegrierter mechatronischer Systeme am Beispiel eines humanoiden Roboters, Forschungsberichte des Instituts für Produktentwicklung, Band 26, Karlsruhe 2007, ISSN 1615-8113.

Hyer, M. W. & Charette, R. F. (1987). *Innovative design of composite structures: use of curvilinear fiber format to improve structural efficiency*, Technical Report 87–5, University of Maryland, College Park, MD, USA, 1987.

Jansson, N. (2007). Optimization of hybrid thermoplastic composite structures using surrogate models and genetic algorithms. Composite Structures, Vol. 80 (2007) No. 1, pp. 21-31.

Jones, R. (1999). *Mechanics of composite materials - 2. ed*, Philadelphia: Taylor & Francis, 1999; ISBN 1-56032-712-X.

Kaneko, K.; Kanehiro, F.; Kajita S.; Hirukawa, H.;Kawasaki, T.; Hirata, M.; Akachi, K.; Isozumi, T. (2004). Humanoid Robot HRP-2, *Proc. IEEE Int. Conference on Robotics and Automation*, pp. 1083-1090, 2004.

Kaneko, K.; Harada, K.; Kanehiro, F.; Miyamori, G.; Akachi, K. (2008). Humanoid Robot HRP-3, *2008 IEEE/RSJ International Conference on Intelligent Robots and Systems*, Acropolis Convention Center Nice, France, Sept, 22-26, 2008.

Kriechbaum, R. (1994). *Ein Verfahren zur Optimierung der Faserverläufe in Verbundwerkstoffen durch Minimierung der Schubspannung nach Vorbildern der Natur*, FZKA 5406, Forschungszentrum Karlsruhe, Eggenstein-Leopoldshafen, Germany, 1994.

Ledermann, M. (2003) Dissertation: *Beiträge zur Optimierung von Faserverbunden nach dem Vorbild der Natur*, Institut für Materialforschung, Forschungszentrum Karlsruhe; Wissenschaftliche Berichte FZKA 6779, ISSN 0947-8620. 2003.

Luo J.H., Gea H.C. (1998) Optimal orientation of orthotropic materials using an energy based method, *Structural Optimization*, Vol. 15 (1998), No. 3/4, pp. 230-236.

Park, I. W.; Kim, J. Y.; Lee, J.; Oh, J. H. (2005). Mechanical Design of Humanoid Robot Platform KHR-3 (KAIST Humanoid Robot – 3: HUBO), *Proc. IEEE-RAS Int. Conference on Humanoid Robots*, pp. 321-326, 2005.

Pedersen, P. (1991). Optimal orientation of anisotropic materials, optimal distribution of anisotropic materials, optimal shape design with anisotropic materials, optimal design for a class of non-linear elasticity, *Optimization of large structural systems; Proceedings of the NATO/DFG Advanced Study Institute* (1991), Berchtesgaden, Germany.

Pedersen, C.B.W. & Allinger, P. (2005) Recent Developments in the Commercial Implementation of Topology Optimization, *TopoptSYMP2005 - IUTAM-Symposium*, Copenhagen, Denmark, pp. 123-132, 2005.

Rosheim, M. (1989). *Robot wrist actuators*, 1. Auflage, 1989 ISBN 0-471-61595-1.

Schulz, S. (2003). *Eine neue Adaptiv-Hand-Prothese auf der Basis flexibler Fluidaktoren*, Dissertation, Fakultät für Maschinenbau, Universität Karlsruhe (TH), 2003.

Schäfer, C. (2000). *Entwurf eines anthropomorphen Roboterarms: Kinematik, Arbeitsraumanalyse, Softwaremodellierung*, Dissertation Fakultät für Informatik, Universität Karlsruhe, 2000.

Setoodeh, S. (2005). Combined topology and fiber path design of composite layers using cellular automata, *Structural and Multidisciplinary Optimization*, Vol. 30 (2005), No. 6, pp. 413-421.

Shadow. www.shadow.org.uk: The Shadow Robot Company.

Wirhed, R. (2001). *Sportanatomie und Bewegungslehre*, Schattauer Verlag, 3. Auflage.

Advances in Robot Manipulators

Edited by Ernest Hall

The purpose of this volume is to encourage and inspire the continual invention of robot manipulators for science and the good of humanity. The concepts of artificial intelligence combined with the engineering and technology of feedback control, have great potential for new, useful and exciting machines. The concept of eclecticism for the design, development, simulation and implementation of a real time controller for an intelligent, vision guided robots is now being explored. The dream of an eclectic perceptual, creative controller that can select its own tasks and perform autonomous operations with reliability and dependability is starting to evolve. We have not yet reached this stage but a careful study of the contents will start one on the exciting journey that could lead to many inventions and successful solutions.

How to reference

In order to correctly reference this scholarly work, feel free to copy and paste the following:

INTECH
open science | open minds